PRAMANA
— journal of
physics

© Indian Academy of Sciences

Vol. 77, No. 2
August 2011
pp. 277–287

Experimental study of the $\pi h_{11/2}$ band in ^{113}Sb

S GANGULY[1,*], P BANERJEE[2], A DEY[3] and S BHATTACHARYA[2]

[1]Department of Physics, Chandernagore College, Chandernagore, Hooghly 712 136, India
[2]Nuclear and Atomic Physics Division, Saha Institute of Nuclear Physics, 1/AF, Bidhan Nagar, Kolkata 700 064, India
[3]Variable Energy Cyclotron Centre, 1/AF, Bidhan Nagar, Kolkata 700 064, India
*Corresponding author. E-mail: sgpresi78@gmail.com

MS received 7 July 2010; revised 2 January 2011; accepted 12 January 2011

Abstract. In the present work, the excited states of ^{113}Sb were populated in the ^{100}Mo(^{20}Ne, $p6n$) reaction at a beam energy of 136 MeV. States only up to 59/2$^-$ were observed in the $\Delta J = 2$ band. Mean lifetimes for the five states (from 4460 to 7998 keV) were measured for the first time using Doppler shift attenuation method. An upper limit of the lifetime (0.14 ps) was estimated for the 9061 keV, 47/2$^-$ state. The $B(E2)$ values, derived from the present lifetime results, correspond to a large quadrupole deformation of $\beta_2 = 0.32$. The observed reduction in the experimental $B(E2)$ values for the 918.4 keV (spin $39/2^- \rightarrow 35/2^-$) and 985 keV (spin $43/2^- \rightarrow 39/2^-$) transitions may be interpreted as due to the proton alignement in the $g_{7/2}$ orbital. The dynamic moment of inertia was observed to be about half of the rigid body value at the highest observed frequency.

Keywords. Nuclear reaction ^{100}Mo(^{20}Ne, $p6n$), $E = 136$ MeV; ^{113}Sb; measured γ-ray energies and intensities; $\gamma\gamma$-coincidences; DCO ratios; Doppler shifts.

PACS Nos 21.10.Re; 21.10.Tg; 25.70.Jj; 27.60.+j

1. Introduction

The low energy states in the nuclei at or near the major shell closure of $Z = 50$ have the expected single-particle structure and have been widely reported in the literature in the past. However, the recent interest in the study of these nuclei centers around the observation of sequences of collective states that have been reported up to fairly high excitation energies and spins. It is understood that these states arise from the excitation of $g_{9/2}$ proton(s) across the closed shell to the down-slopping $g_{7/2}d_{5/2}$ Nilsson orbitals giving rise to particle–hole configurations.

The single-particle states in the odd-A antimony nuclei ($Z = 51$) represent the coupling of the valence proton in the $g_{7/2}$, $d_{5/2}$ and $h_{11/2}$ orbitals to the spherical Sn ($Z = 50$) core states. The collective states in these nuclei have been interpreted to arise from (i) a 2p-1h $\pi(g_{7/2})^2 \otimes \pi(g_{9/2})^{-1}$ configuration, resulting from the excitation of a $g_{9/2}$ proton across

DOI: 10.1007/s12043-011-0103-6; *e*Publication: 9 July 2011

the $Z = 50$ shell gap leading to $\Delta I = 1$ bands and (ii) the coupling of the odd proton and the neutrons in the $h_{11/2}$, $g_{7/2}$ and $d_{5/2}$ orbitals to the 2p-2h deformed core states of tin that result from the de-excitation of two protons from the high-Ω $g_{9/2}$ orbital to the low-Ω $g_{7/2}$ and $d_{5/2}$ orbitals. The latter scheme leads to decoupled $\Delta J = 2$ bands.

Several nuclei at or near the major shell closure of $Z = 50$ have shown exotic collective structures that co-exist with the expected single-particle states. The low-energy states of these nuclei in this mass region arise from the 2 particle-2 hole (2p-2h) proton configuration where a pair of $g_{9/2}$ protons are excited across the $Z = 50$ closed shell to the down-slopping $g_{7/2}d_{5/2}$ Nilsson orbitals. Rotational intruder bands based on such 2p-2h configuration $\pi(g_{9/2})^2 \otimes \pi(g_{7/2})^{-2}$ are reported in several Sn, Sb and Te isotopes in this mass region. The odd-mass Sb isotopes are interpreted to arise from the coupling of the last odd-proton in the $\pi(h_{11/2})$ orbital to the neighbouring even–even Sn 2p-2h cores. The neutrons outside the ^{100}Sn core are also distributed in the same orbitals with some occupying the $h_{11/2}$ shell. Some of these bands have been observed to terminate in a non-collective oblate state at high spin where the final states are formed, usually at a large energy cost.

Afanasjev *et al* [1] have identified 40 bands in 18 nuclei in this mass region, with well-defined configurations that are expected to exhibit band termination. Experimentally, rotational bands have been observed up to high spins in several Sn, Sb and Te isotopes [2–4]. Some of these bands have been interpreted in terms of configuration-dependent cranked Nilsson–Strutinsky calculations that predict a gradual change from collective prolate at low spin to non-collective oblate at high spin, leading to smooth band termination. A characteristic feature of such bands is a large decrease in their dynamic moment of inertia ($J^{(2)}$), to approximately a third of the rigid-body value, as the rotational frequencies approach 1 MeV/$\hbar$. More recently, lifetime studies in ^{108}Sn and ^{109}Sb have shown a smooth decline in $B(E2)$ values with spin for the higher lying states [5]. This has been interpreted as due to a gradual change in the shape of the nucleus from collective prolate at low spins to a non-collective oblate at high spins, associated with the alignment of the angular momentum vectors of the valance nucleons with the rotational axis.

The low-lying excited states in Sb nuclei ($Z = 51$) show single-particle behaviour. The valance proton in $g_{7/2}$, $d_{5/2}$ and $h_{11/2}$ orbitals coupled to the spherical even Sn ($Z = 50$) core, are responsible for this behaviour. However, the high spin states are dominated by rotational behaviour. These rotational states arise as a result of the coupling of the valance proton occupying $g_{7/2}$, $d_{5/2}$ and $h_{11/2}$ orbitals with 2p-2h deformed Sn states. In a recent study of ^{113}Sb, Janzen *et al* [6] observed a rotational band up to a spin of $75/2^-$ and excitation energy of about 19 MeV based on $\pi h_{11/2}$ configuartion. An extracted average value of the transition quadrupole moment Q_t of 4.4 ± 0.6 [6] was also determined using the centroid shift method for this rotational band. However, lifetime results for the individual states are not known in this rotational band. In the present work, lifetime has been measured for the first time for the five excited states belonging to this rotational band in order to understand the structures of the states.

2. Experimental method

High spin states of ^{113}Sb were populated in the ^{100}Mo(^{20}Ne, $p6n$) reaction at a beam energy of 136 MeV at the Variable Energy Cyclotron Centre, Kolkata, India. The target consisted of isotopically enriched (99.5%) ^{100}Mo, 4.7 mg/cm^2 thick, evaporated on an aluminium backing. Two and higher fold $\gamma\gamma$-coincident events were collected using an array of six Compton-suppressed Clover detectors belonging to the Indian National Gamma Array (INGA) with the detectors arranged in three groups of two detectors each, at 40°, 90° and 125° angles with respect to the beam direction. The raw data were sorted in different 4096×4096 matrices after gain matching of all the spectra to a dispersion of 1 keV per channel. The detectors had an energy resolution of 2.1 keV at 1332 keV and relative efficiencies of about 40%. The energy calibration was obtained from the energies of the known γ-ray lines in ^{111,112}Sn in the spectrum. The spectra for lifetime analysis using the Doppler shift attenuation (DSA) technique were obtained from matrices generated from coincidences between the forward and backward angle events with those in the remaining detectors. The data were analysed using the computer code INGASORT [7]. The directional correlation of oriented nuclei (DCO) ratios for assigning γ-ray multipolarity were determined from a matrix with events recorded at 90° along one axis and those at 125° along the other. Other relevant experimental details are available in ref. [8]. The lifetimes of the excited states were extracted from the DSA data using the analysis package LINESHAPE [9]. The details of the slowing down history of the recoils (moving with an initial recoil velocity of $\beta = 0.0201$) in the target and backing were simulated using a Monte Carlo technique, which involved 10,000 histories with a time step of 0.002 ps, and the

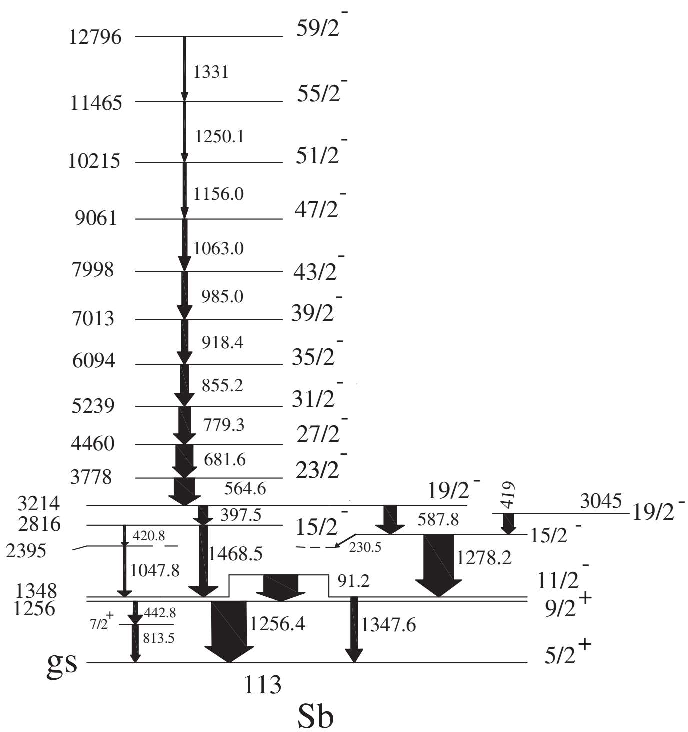

Figure 1. Level scheme of ^{113}Sb obtained in the present work.

results were sorted according to detector geometry. The shell-corrected stopping powers of Northcliffe–Schilling [10] were used. The fitting process was started with the highest observed transition with adequate statistics (in this case the 1063 keV transition depopulating the 9061 keV state) and considering that the feeding time information to this state has large uncertainties, only an effective lifetime (stated as the upper limit) was determined. This was then used as an input parameter for the estimation of the lifetimes of the lower lying states in the band. The side-feeding times (τ_{sf}) used in the analysis of the data for ^{113}Sb were constrained to be similar to those used in the analysis for ^{112}Sn [8]. The τ_{sf} value was about 0.1 ps for a state with an excitation energy of 9 MeV and followed the general trend that they increased with decrease in excitation energy. Side-feeding intensities, used in the present analyses, were obtained from the γ-ray relative intensities measured at 125° to the beam from the spectra gated mostly by the 91.2, 397.5, 587.8, 1256.4 and 1278.2 keV transitions (see figure 1). A 50% uncertainty for these τ_{sf} values along with the statistical uncertainties were considered while assigning the errors to the level lifetimes.

3. Experimental results and discussion

The level scheme of ^{113}Sb, deduced from the present work, is shown in figure 1. Only the negative-parity rotational band and the lower-lying states to which the band decays are shown in the figure. The placement of all transitions in the level scheme up to an excitation energy of 12796 keV and spin $59/2^-$ is confirmed in this work. The spectrum

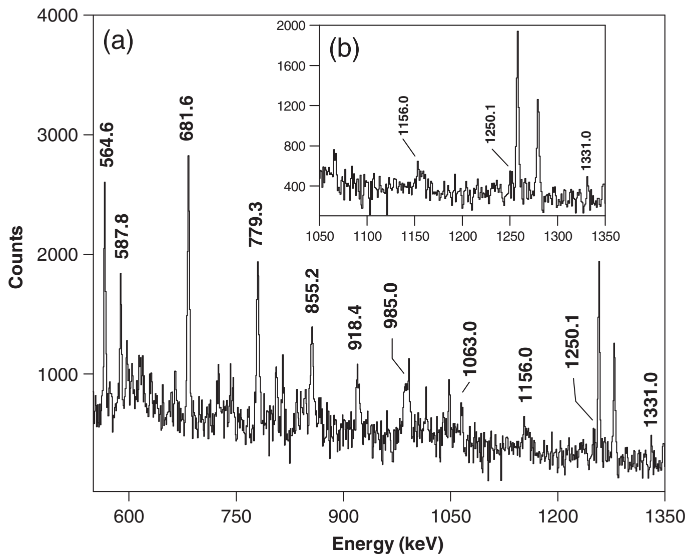

Figure 2. (**a**) Partial γ-ray spectrum gated by 91.2 + 397.5 + 564.6 + 587.8 + 1256.4 + 1278.2 keV transitions projected at 90° to the beam direction. (**b**) Inset shows the higher-lying transitions projected at 90°.

gated by the 91.2, 397.5, 564.6, 587.8, 1256.4 and 1278.2 keV transitions is shown in figure 2 in support of the placement of γ-rays in the level scheme. The energies of the in-band transitions observed in the present work are in agreement with the earlier reports [6,11] except for the highest transition (with 1331 keV energy). Indication of the higher-lying transitions in this band cannot be found in the present work. The results on the relative intensities of the transitions and the DCO ratio of the transitions (belonging to the $\pi h_{11/2}$ band) are presented in table 1. Although the level scheme of ^{113}Sb has been reported up to high spins as stated earlier, information on the γ-ray relative intensities and their branching ratios are incomplete. Present branching ratios for the 1256 and 1348 keV levels are consistent with the earlier results. Gamma-ray branchings of 2±0.56 and 98±7, 18.8±2 and 81.2±0.11, 43.9±4.8 and 56.1±6.8 have also been determined for the 2626, 2816 and 3214 keV states for which no information is available in the literature [12]. Present DCO measurement confirms the $E2$ nature of the transitions upto 55/2$^-$. Level lifetimes (τ), the $B(E2)$ rates, the transition quadrupole moments (Q_t) and the quadrupole deformations (β_2) for the $\Delta J = 2$ deformed band in ^{113}Sb are summarized in table 2. The

Table 1. Present experimental results on level energies (E_x), γ-ray energies (E_γ), γ-ray relative intensities and the DCO ratios (only for the $\pi h_{11/2}$ band) in ^{113}Sb.

E_x (keV)	E_γ (keV)	$J_i^\pi \rightarrow J_f^\pi$	I_γ	Gate	R_{DCO}
814	813.5	$7/2^+ \rightarrow 5/2^+$	20±5		
1256	442.8	$9/2^+ \rightarrow 7/2^+$	16±3		
	1256.4	$9/2^+ \rightarrow 5/2^+$	100±3		
1348	91.2	$11/2^- \rightarrow 9/2^+$	99±6		
	1347.6	$11/2^- \rightarrow 5/2^+$	20±2		
2395	1047.8	$13/2^+ \rightarrow 11/2^-$	8±1		
2626	230.5	$15/2^- \rightarrow 13/2^+$	2±1		
	1278.2	$15/2^- \rightarrow 11/2^-$	85±4		
2816	420.8	$15/2^- \rightarrow 13/2^+$	6±0.4		
	1468.5	$15/2^- \rightarrow 11/2^-$	24±2		
3045	419	$19/2^- \rightarrow 15/2^-$	25±6		
3214	397.5	$19/2^- \rightarrow 15/2^-$	28±2		
	587.8	$19/2^- \rightarrow 15/2^-$	36±4		
3778	564.6	$23/2^- \rightarrow 19/2^-$	59±6	1468.5	1.08±0.11
4460	681.6	$27/2^- \rightarrow 23/2^-$	49±3.5	1468.5	1.04±0.09
5239	779.3	$31/2^- \rightarrow 27/2^-$	33±4	564.6	1.08±0.13
6094	855.2	$35/2^- \rightarrow 31/2^-$	24±3	564.6	1.14±0.16
7013	918.4	$39/2^- \rightarrow 35/2^-$	19±4	564.6	1.10±0.23
7998	985.0	$43/2^- \rightarrow 39/2^-$	16±4	681.6	1.10±0.30
9061	1063.0	$47/2^- \rightarrow 43/2^-$	13±3.0	681.6	1.12±0.25
10215	1156.0	$51/2^- \rightarrow 47/2^-$	11±3	681.6	1.16±0.30
11465	1250.1	$55/2^- \rightarrow 51/2^-$	6±2	681.6	1.06±0.33
12795.8	1331	$59/2^- \rightarrow 55/2^-$	5±1		

Table 2. Present experimental results on mean lifetime (τ), $B(E2)$, transition quadrupole moments (Q_t) and quadrupole deformation (β_2) for negative-parity rotational band in ^{113}Sb.

E_γ (keV)	Spin $J_i^\pi \to J_f^\pi$	τ (ps)	$B(E2)$ (W.u.)	Q_t (eb)	β_2
681.6	$27/2^- \to 23/2^-$	0.84±0.03	204±7	4.38±0.11	0.30±0.01
779.3	$31/2^- \to 27/2^-$	0.51±0.02	174±6	4.03±0.10	0.27±0.01
855.2	$35/2^- \to 31/2^-$	0.17±0.01	319±14	5.43±0.17	0.36±0.01
918.4	$39/2^- \to 35/2^-$	0.14±0.01	284±18	5.11±0.23	$0.34^{+0.02}_{-0.01}$
985.0	$43/2^- \to 39/2^-$	0.12±0.01	226^{+19}_{-17}	$4.54^{+0.27}_{-0.24}$	0.31±0.01
1063.0	$47/2^- \to 43/2^-$	<0.14	>139	>3.55	>0.24

reduced transition strength $B(E2)$ and the transition quadrupole moment Q_t were obtained from the lifetimes using the formula

$$B(E2) = \frac{8.20 \times 10^{-10}}{E_\gamma^5 \tau}\ \mathrm{e^2fm^4},$$

where τ is the lifetime (in second) of the state and E_γ is the transition energy (in MeV) and

$$B(E2, J \to J-2) = \frac{5}{16\pi} Q_t^2 \langle J2K0|J-2K\rangle^2,$$

where $B(E2)$ is in e^{2}b^2 and quadrupole moment Q_t is in eb and the term in brackets is Clebsch–Gordon coefficient. K is the projection of total angular momentum on the symmetry axis. Although the average transition quadrupole moment and the quadrupole deformation for this band have been reported previously [6] from DSA data using centroid shift method, lifetimes of individual states are reported for the first time in the present work. Mean lifetimes of 0.84±0.03, 0.51±0.02, 0.17±0.01, 0.14±0.01 and 0.12±0.01 ps have been measured for the five states with energies 4460, 5239, 6094, 7013 and 7998 keV respectively, from the line-shape analysis of DSA data in the present work. In addition, an upper limit of mean life of 0.14 ps has been estimated for the 9061 keV state. The results are summarized in table 2. The observed line shapes, together with the theoretical fits generated using the computer package LINESHAPE [9] are presented in figures 3 and 4. The line shapes for the 681.6, 779.3, 855.2 and 918.4 keV transitions observed at 40° and 125°, together with the theoretical fits are shown in figures 3 and 4. The spectra at 90° to the beam are also included in the figure. The fitted line shapes are shown by red solid lines and the contaminant lines are shown by dotted lines (see the upper two panels of figures 4a and 4b). The present lifetime results lead to a large average quadrupole deformation of $\beta_2 = 0.32$ and transition quadrupole moment $Q_t = 4.70\pm0.50$ eb. This result is consistent with the average quadrupole moment reported in [6].

The low-energy states in ^{113}Sb ($Z = 51$) have single-particle character arising from the coupling of the proton $g_{7/2}$, $d_{5/2}$ and $h_{11/2}$ orbitals to the spherical Sn core states. Deformed structures have however also been observed in ^{113}Sb and several other Sb isotopes as in the

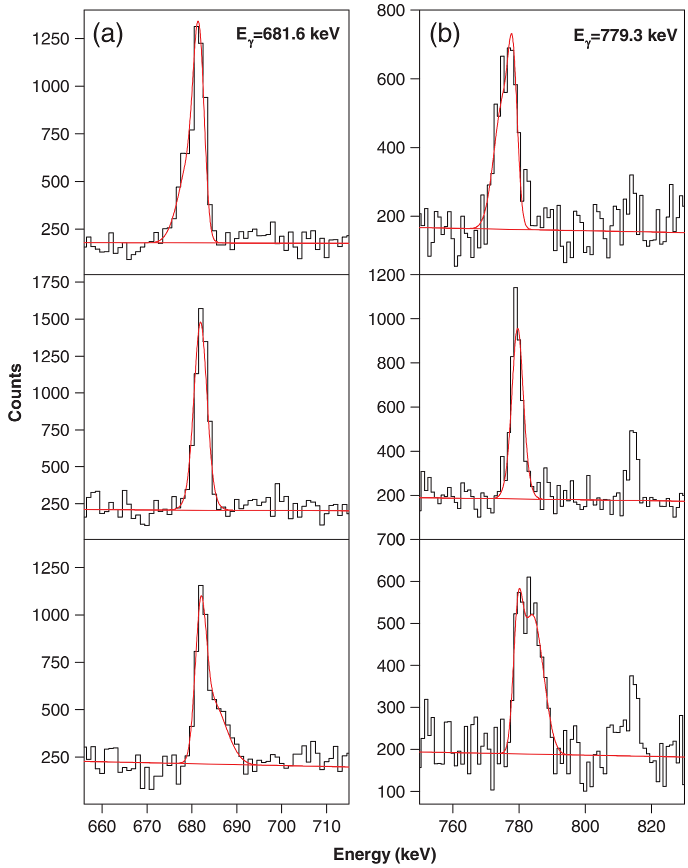

Figure 3. DSA spectra for $E_\gamma = 681.6$ and 779.3 keV in band 1, gated by low-lying transitions in the band for ^{113}Sb. The upper, middle and lower panels, respectively show the spectra at 125°, 90° and 40° to the beam direction. The red lines indicate the transition line shape.

neighbouring ^{111,112}Sn nuclei. These include the $\Delta J = 1$ collective bands in the odd-A Sb isotopes with $N = 58$–68, based on the 2p-1h configuration $\pi(g_{7/2})^2 \otimes (g_{9/2})^{-1}$ [13], and the decoupled $\Delta J = 2$ deformed bands in $^{109-111,113-115,117,119}$Sb [6,14–20], interpreted as resulting from the coupling between the valence nucleons in the $g_{7/2}$, $d_{5/2}$ and $h_{11/2}$ orbitals and the 2p-2h deformed core Sn states. In ^{113}Sb, Janzen *et al* [6] reported this band, based on the proton $h_{11/2}$ orbital coupled to the 2p-2h deformed core, up to a spin of $75/2^-$. The present work provides a detailed study of this band. Although Janzen *et al* have reported the band up to $75/2^-$, states only up to $J^\pi = 59/2^-$ could be observed in this intruder $\pi h_{11/2}$ band in the present work. The plot of dynamic moment of inertia (J^2) with rotational frequency, shown in figure 5, indicates that alignments take place at $\hbar\omega = 0.46$ and 0.69 MeV. The increase in aligned angular momenta (i_x), corresponding to these alignments, are calculated to be about $7.5\hbar$ and $4.5\hbar$, and the corresponding interaction strengths are calculated to be about 360 and 210 keV, respectively. The first band crossing is due to

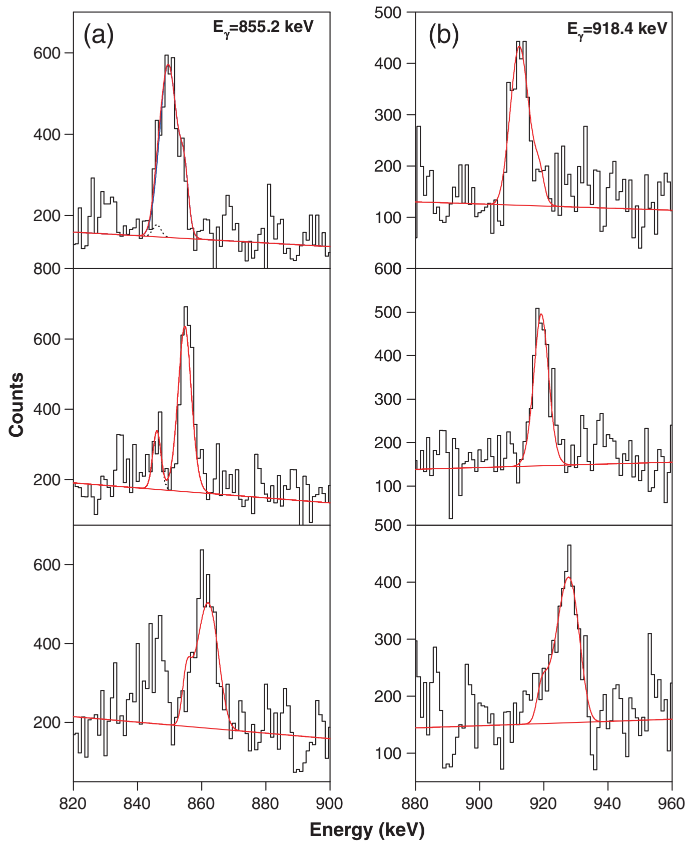

Figure 4. DSA spectra for $E_\gamma = 855.2$ and 918.4 keV in band 1, gated by low-lying transitions in the band for ^{113}Sb. The upper, middle and lower panels, respectively show the spectra at 125°, 90° and 40° to the beam direction. The red line indicates the transition line shape and the dotted lines indicate the contaminated peaks.

the rotational alignment of a pair of $h_{11/2}$ neutrons [6]. Cranked-shell-model calculations have been performed in the present work using a modified harmonic oscillator potential. Quasiparticle Routhians, calculated with a quadrupole deformation of $\beta_2 = 0.32$ (obtained experimentally in the present work) and $\gamma = 0°$ (hexadecapole deformation was assumed to be zero) also show that the first band crossing is due to the alignment of a pair of $h_{11/2}$ neutrons and occurs at a frequency $\hbar\omega \sim 0.45$ MeV. The first crossing however occurs at a frequency 0.09 MeV higher relative to the core nucleus ^{112}Sn and with a larger interaction strength than the known neutron $h_{11/2}$ alignments in ^{110,112,114}Sn [8,21,22]. The reduction in the experimental $B(E2)$ values for the 918.4 keV (spin $39/2^- \rightarrow 35/2^-$) and 985.0 keV (spin $43/2^- \rightarrow 39/2^-$) transitions is consistent with the first alignment. The second crossing is associated with the rotational alignment of $g_{7/2}$ protons. The delayed neutron $h_{11/2}$ alignment and the large interaction strength signify large residual interaction between the valance high j-neutrons and protons.

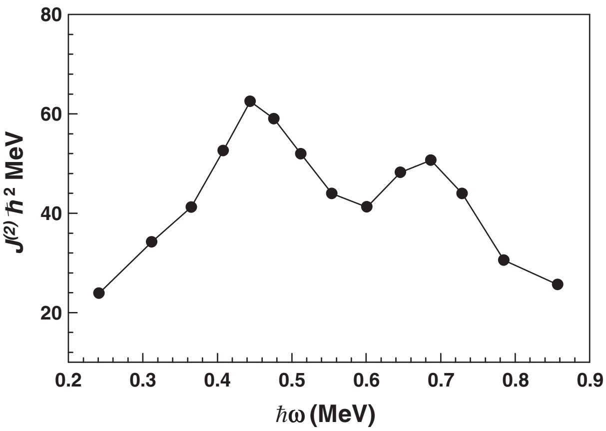

Figure 5. Plot of dynamic moment of inertia (J^2) vs. frequency ($\hbar\omega$) for the $\pi h_{11/2}$ band in ^{113}Sb.

The deformation obtained for the band is the largest reported in this mass region with Z close to the shell-closure. The explanation for this large deformation of the states of the intruder band in ^{113}Sb possibly lies in the strong residual p–n interaction and the occupation of the high-j intruder orbital (in this case the $h_{11/2}$) that drives the system towards a large deformation. A comparison of the deformations estimated for the intruder bands in the two $N = 62$ isotones (^{112}Sn and ^{113}Sb) would lend a strong support to this interpretation. However, Janzen *et al* [6] have pointed out that the intruder band in ^{111}In (also with $N = 62$), with a $h_{11/2}$ proton coupled to a 0p-2h $(g_{7/2})^0 \otimes (g_{9/2})^{-2}$ deformed core, has been reported to have a moderate quadrupole deformation of $\beta_2 = 0.18$ whereas the band in ^{113}Sb with a $h_{11/2}$ proton coupled to a 2p-2h $(g_{7/2})^2 \otimes (g_{9/2})^{-2}$ deformed core has a large β_2 value of 0.32. This suggests that it is the 2p-2h core configuration, which remains intact in ^{113}Sb but not in ^{111}In, along with the $h_{11/2}$ proton, that plays a major role in contributing to large core deformation. The significant decrease in the $B(E2)$ value for the 918.4 keV, $39/2^- \rightarrow 35/2^-$ and 985 keV, $43/2^- \rightarrow 39/2^-$ transitions are consistent with the observation of the $h_{11/2}$ neutron alignment at a rotational frequency of $\hbar\omega \sim 0.46$ MeV. The configuration $\pi(g_{9/2})^{-2} \otimes (g_{7/2})^2 \otimes \pi(h_{11/2}) \otimes \nu(h_{11/2})^4$ has been proposed for the intruder band in ^{113}Sb, following the alignment of a $h_{11/2}$ neutron pair [1,23]. The previous total Routhian surface (TRS) calculations by Satula and Wyss [24], for the $\pi h_{11/2}$ band in ^{113}Sb indicate that at low frequencies, the states have a fairly large near prolate deformation and with increase in rotational frequency, the shape is driven towards smaller β_2 and large positive γ-values. The structure therefore becomes less collective with increase in spin.

The $\pi h_{11/2}$ intruder band in ^{113}Sb has been previously identified as a possible candidate for exhibiting the phenomenon of band termination [1]. The $[21,4]^-$ configuration (following the notation introduced by Afanasjev and Ragnarsson [25]) gives rise to a terminating spin of $95/2^-$ as a result of the aligning of the spins of all the particles and holes outside the core ^{100}Sn. The band needs to be studied up to spins higher than those observed in the present work ($J^\pi = 59/2^-$) or reported in the literature ($75/2^-$) and lifetimes of such excited states have to be measured in order to arrive at a firm conclusion regarding band termination.

Acknowledgements

The authors thank the members of the INGA collaboration group for setting up the array at the VECC, Kolkata. Thanks are due to the staff of the Cyclotron and the Target Laboratory at the VECC, Kolkata, for their cooperation. One of the authors (SG) was supported partially by the UGC-DAE-CSR-KC vide project number UGC-DAE-CSR-KC/CRS/2009/NP05/1353.

References

[1] A V Afanasjev, D B Fossan, G J Lane and I Ragnarsson, *Phys. Rep.* **322**, 1 (1999)
[2] R Wadsworth, H R Andrews, C W Beausang, R M Clark, J. DeGraaf, D B Fossan, A Galindo-Uribarri, I M Hibbert, K Hauschild, J R Hughes, V P Janzen, D R LaFosse, S M Mullins, E S Paul, L Persson, S Pilotte, D C Radford, H Schnare, P Vaska, D Ward, J N Wilson and I Ragnarsson, *Phys. Rev.* **C50**, 483 (1994)
[3] G J Lane, D B Fossan, C J Chiara, H Schnare, J M Sears, J F Smith, I Thorslund, P Vaska, E S Paul, A N Wilson, J N Wilson, K Hauschild, I M Hibbert, R Wadsworth, A V Afanasjev and I Ragnarsson, *Phys. Rev.* **C58**, 127 (1998)
[4] I Thorslund, D B Fossan, D R LaFosse, H Schnare, K Hauschild, I M Hibbert, S M Mullins, E S Paul, I Ragnarsson, J M Sears, P Vaska and R Wadsworth, *Phys. Rev.* **C52**, 2839R (1995)
[5] R Wadsworth, R M Clark, J A Cameron, D B Fossan, I M Hibbert, V P Janzen, R Krücken, G J Lane, I Y Lee, A O Macchiavelli, C M Parry, J M Sears, J F Smith, A V Afanasjev and I Ragnarsson, *Phys. Rev. Lett.* **80**, 1174 (1998)
[6] V P Janzen, H R Andrews, B Haas, D C Radford, D Ward, A Omar, D. Prévost, M Sawicki, P Unrau, J C Waddington, T E Drake, A Galindo-Uribarri and R Wyss, *Phys. Rev. Lett.* **70**, 1065 (1993)
[7] R K Bhowmik, INGASORT Manual, Private Communication (2003)
[8] S Ganguly, P Banerjee, I Ray, R Kshetri, R Raut, S Bhattacharya, M Saha-Sarkar, A Goswami, S Mukhopadhyay, A Mukherjee, G Mukherjee and S K Basu, *Nucl. Phys.* **A789**, 1 (2007)
[9] J C Wells and N Johnson, *Rep. ORNL* **6689**, 44 (1991)
[10] L C Northcliffe and R F Schilling, *Nucl. Data Tables* **7**, 233 (1970)
[11] C-B Moon, C S Lee, J C Kim, J H Ha, T Komatsubara, T Shizuma, K Uchiyama, K Matsuura, M Murasaki, Y Sasaki, H Takahashi, Y Tokita and K Furuno, *Phys. Rev.* **C58**, 1833 (1998)
[12] Jean Blachot, *Nucl. Data Sheets* **100**, 179 (2003)
[13] R E Shroy, A K Gaigalas, G Schatz and D B Fossan, *Phys. Rev.* **C19**, 1324 (1979)
[14] H Schnare *et al*, *Phys. Rev.* **C54**, 1598 (1996)
[15] G J Lane, D B Fossan, I Thorslund, P Vaska, R G Allatt, E S Paul, L Kaübler, H Schnare, I M Hibbert, N OBrien, R Wadsworth, W Andrejtscheff, J de Graaf, J Simpson, I Y Lee, A O Macchiavelli, D J Blumenthal, C N Davids, C J Lister, D Seweryniak, A V Afanasjev and I Ragnarsson, *Phys. Rev.* **C55**, R2127 (1997)
[16] D R LaFosse, D B Fossan, J R Hughes, Y Liang, H Schnare, P Vaska, M P Waring, J-y Jhang, R M Clark, R Wadsworth, S A Forbes, E S Paul, V P Janzen, A Galindo-Uribarri, D C Radford, D Ward, S M Mullins, D Prevost and G Zwartz, *Phys. Rev.* **C50**, 1819 (1994)
[17] E S Paul, V P Janzen, D C Radford, D Ward, S M Mullins, D B Fossan, D R Lafosse, H Schnare, H Timmers, P Vaska, R M Clark and R Wadsworth, *Phys. Rev.* **C50**, 2297 (1994)
[18] C-B Moon, S J Chae, J H Ha, T Komatsubara, J Lu, T Hayakawa and K Furuno, *Z. Phys.* **A352**, 245 (1995)
[19] R S Chakrawarthy and R G Pillay, *Phys. Rev.* **C54**, 2319 (1996)

[20] D R LaFosse, D B Fossan, J R Hughes, Y Liang, H Schnare, P Vaska, M P Waring and J-y Zhang, *Phys. Rev*. **C56**, 760 (1997)
[21] H Harada, T Murakami, K Yoshida, J Kasagi, T Inamura and T Kubo, *Phys. Lett.* **B207**, 17 (1988)
[22] J Gableske, A Dewald, H Tiesler, M Wilhelm, T Klemme, O Vogel, I Schneider, R Peusquens, S Kasemann, K O Zell, P von Brentano, P Petkov, D Bazzacco, C Rossi Alvarez, S Lunardi, G de Angelis, M de Poli and C Fahlander, *Nucl. Phys.* **A691**, 551 (2001)
[23] D B Fossan, *Proceedings of the Workshop on Gammasphere Physics,* Berkley, Dec 1–2, 1995, (World Scientific, Singapore, 1996) p. 186.
[24] W Satula and R Wyss, *Phys. Scr.* **T56**, 159 (1995)
[25] A V Afanasjev and I Ragnarsson, *Nucl. Phys.* **A591**, 387 (1995)